

NOAA ROSES Semi-Annual Report

Reporting Period: September 2020 – February 2021 (1st report)

PI: Prof. Ping Yang (Texas A&M University)

Co-PI(s): Prof. Xianglei Huang (University of Michigan)

Project Title: Utilizing geostationary satellite observations to develop a next generation ice cloud optical property model in support of JCSDA Community Radiative Transfer Model (CRTM) and JPSS CAL/VAL

Executive Summary (1 paragraph max)

This semi-annual report contains two parts: the first part summarizes of the research progress of the Texas A&M University team led by Prof. Ping Yang, and the second part summarizes of the research progress of the University of Michigan Co-I, Prof. Xianglei Huang.

Progress toward FY20 Milestones and Relevant Findings (with any Figs)

During the first 6-month period from August 1st, 2020 to January 31st, 2021, we have made the following progress for Task 1 and Task 2 as summarized below:

Task 1: Determination of the next-generation ice optical property model

- Literature survey on the particle shapes and optical properties of ice crystals in the atmosphere;
- Sensitivity tests for various ice particle shapes;
- Determination of the ice particle shapes as part of the next-generation ice optical property model.

Although most atmospheric radiative transfer applications involving ice clouds assume a spatially invariant single ice crystal habit, many aircraft in-situ observations confirm that dominant ice crystal shapes have substantial variations with ambient air temperature and other environmental factors.

Korolev et al. (2003) investigated the morphological characteristics of ice crystals based on aircraft in-situ measurements with a cloud particle imager (CPI) during the Third Canadian Freezing Drizzle Experiment (CFDE III) campaign conducted in the Great Lakes Region from December 1997 to February 1998. They investigated the temperature dependence and size dependence of the “roundness”, defined as the ratio of particle projected area to the circumscribed sphere projected area, and aspect ratio, defined as the ratio of the minor axis to the major axis of a particle obtained from a CPI mage analysis. It was found that the average roundness rapidly decreases from 0.9 to 0.6 as size increases from 20 to 80 μm , slowly decreases from 0.6 to 0.4 for larger sizes, and is almost independent of temperature. The aspect ratio changes from 0.8 to 0.6 as the temperature increases from -40 to 0 $^{\circ}\text{C}$ for crystal sizes > 60 μm . For smaller sizes, the size dependence is more pronounced. The aspect ratio

varies from 0.8 to 0.7 as particle sizes increase from 25 μm to 60 μm . The standard deviations of the roundness and aspect ratio are about 0.1.

Um et al. (2015) summarized statistics of ice particle habits and their aspect ratios obtained from multiple aircraft in-situ observations conducted in the tropics, mid-latitudes, and Arctic regions. The analysis focuses on pristine ice crystals that have distinct particle shapes. However, the majority of particles ($\sim 90\%$) are undetermined or irregular shapes. Among pristine particles, single column particles appear throughout the temperature range. The fraction of single column particles is 40.9% in the tropics, 48.3% in midlatitudes, and 70.7% in Arctic regions, while plate particle fractions are 43.5%, 10.8%, and 9.2%, respectively, with higher fractions at $-40 < T < -20^\circ\text{C}$. Aspect ratios of pristine particles are $2.1\text{--}2.5 \pm 1.0$ at $-67 < T < -35^\circ\text{C}$ and $2.3\text{--}2.45 \pm 0.8$ at $-40 < T < -15^\circ\text{C}$ for columns, and 0.25 ± 0.17 and $0.22\text{--}0.3 \pm 0.08$ for plates respectively, showing a weak temperature dependence. The particle habits depend largely on their origin of clouds: Anvil clouds contain more plate particles (38.6–60.2%) than non-anvil clouds (5.2–6.5%).

Ice particle irregularity (or complexity) is also important. Magee et al. (2020) conducted balloon-borne imaging observations of ice crystals in cirrus clouds, revealing that a variety of ice crystal shapes rather than several major particle shapes were observed. Among these ice crystal shapes, 86% of ice crystals were highly complex and thereby undetermined particle shapes. Multiple scales (sub-microns to hundreds of microns) of ice crystal surface textures on cloud ice particles were observed in April 24, 2018 when a faint 22° halo was observed and cloud temperature was -40 to -55°C . Other major particle shapes are columns (4%), bullet rosette (4%), and plates (1.5%) with their mean and median aspect ratios of 2.39 and 2.29, 1.84 and 1.6, and 1.64 and 1.56, respectively. Small-scale surface texture affects optical properties of ice crystals. Zhang et al. (2016) demonstrated that the degree of surface roughness conceptually defined by Yang and Liou (1998) has a physical relation with ice surface growth through diffusion and evaporation randomly to the surface-normal directions based on the Kardar–Parisi–Zhang (KPZ) equations with a nonlinear term omitted. Single-scattering property computations of surface roughened particles reveal that roughness has nonnegligible effects for size parameters $kD > 20$. Voigtländer et al. (2018) demonstrate that ice crystal surface texture and particle irregularity can increase more rapidly with higher ice supersaturation, based on laboratory measurements. Also, the depositional growth–sublimation process due to a cyclic relative humidity oscillation can contribute to a gradual increase of the roughness and irregularity of an ice crystal.

Since the small-scale surface roughness and aspect ratio have substantial impacts on the optical properties of ice crystals, we will take into account these two variables in the next-generation ice optical property model. In addition, to simulate complex aggregate particles, we will consider an irregularly distorted hexagonal column aggregate model (e.g., Loeb et al., 2018). The knowledge of the reported ice crystal shapes obtained through our literature survey will be used to perform an ice crystal morphological consistency check of the next-generation ice optical property model.

To model the optical properties of realistic ice crystals, we performed sensitivity tests with a focus on modeling the surface roughness. Currently available ice optical property databases (e.g., Yang et al., 2013) consider the degree of surface roughness for large ice crystals where the surface texture plays an essential role in single-scattering properties. Previous research has generally considered the surface roughness effects of small size parameter particles (e.g., $kD < 30$) to be negligible. We revisit the sensitivity of the surface texture on the single-scattering properties of ice crystals, using state-of-the-art rigorous light scattering computational capabilities, to seek better surface texture modeling for ice crystals.

Figure 1 shows the particle shapes used for the sensitivity tests. The size parameter of these ice crystals is 100, defined as the maximum diameter of the circumscribed sphere of the particle. We use the face-tilting approach (Liu et al., 2013) to model the surface texture of ice crystals. The aspect ratio of these ice crystals is unity. In contrast to the definition of the surface roughness (s_2) used for large ice crystals in geometric-optics methods (Yang and Liou, 1998), we consider the relative scale of the surface roughness through discretization of the faces in the surface-tilting process. The maximum length of each discretized face (D_{face}) ranges from $D/10$ to $D/160$.

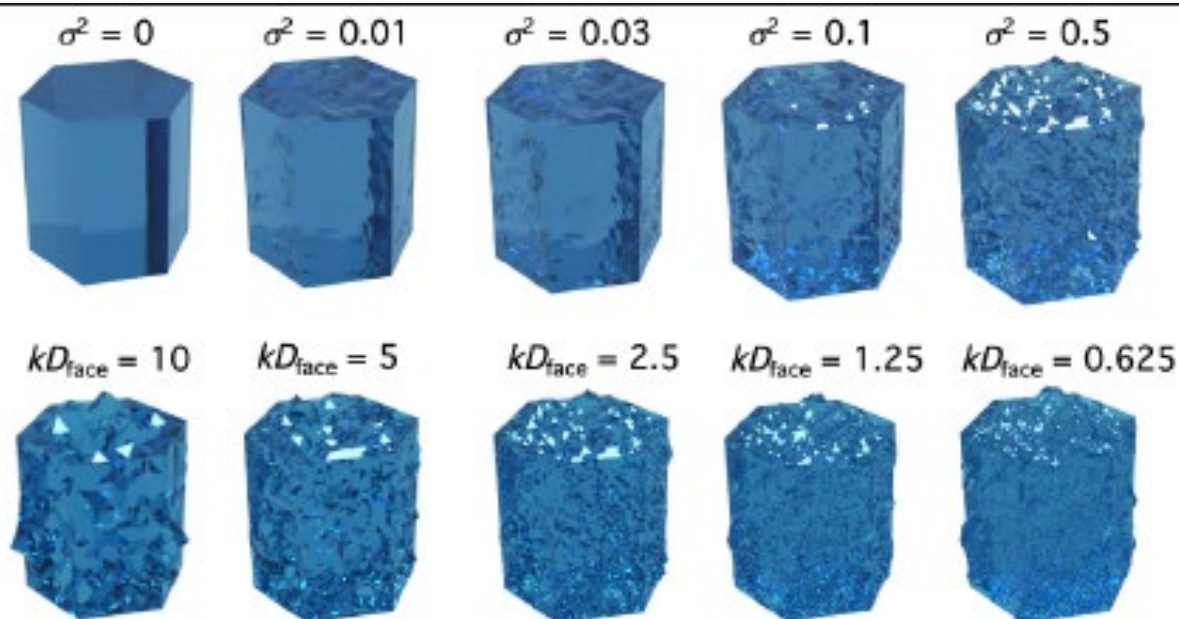


Figure 1. Hexagonal column particles with size parameter 100. The upper row shows hexagonal columns with various degrees of surface roughness with a scale of $D/40$, and the lower row shows columns with $s_2 = 0.5$ and various scales of surface roughness.

Figure 2 demonstrates the sensitivity of the phase matrix elements to the surface roughness. As indicated by previous studies, a small degree of surface roughness has a large impact on the phase matrix elements, which confirms that necessity of a relevant modeling of the surface roughness. Note that the size parameter of 100 in the present definition corresponds to $kL \sim 71$, where L is the maximum length of an axis (Bi and Yang, 2014), and therefore the particle does not have the 22° halo peak that should be pronounced for $kL > 80$.

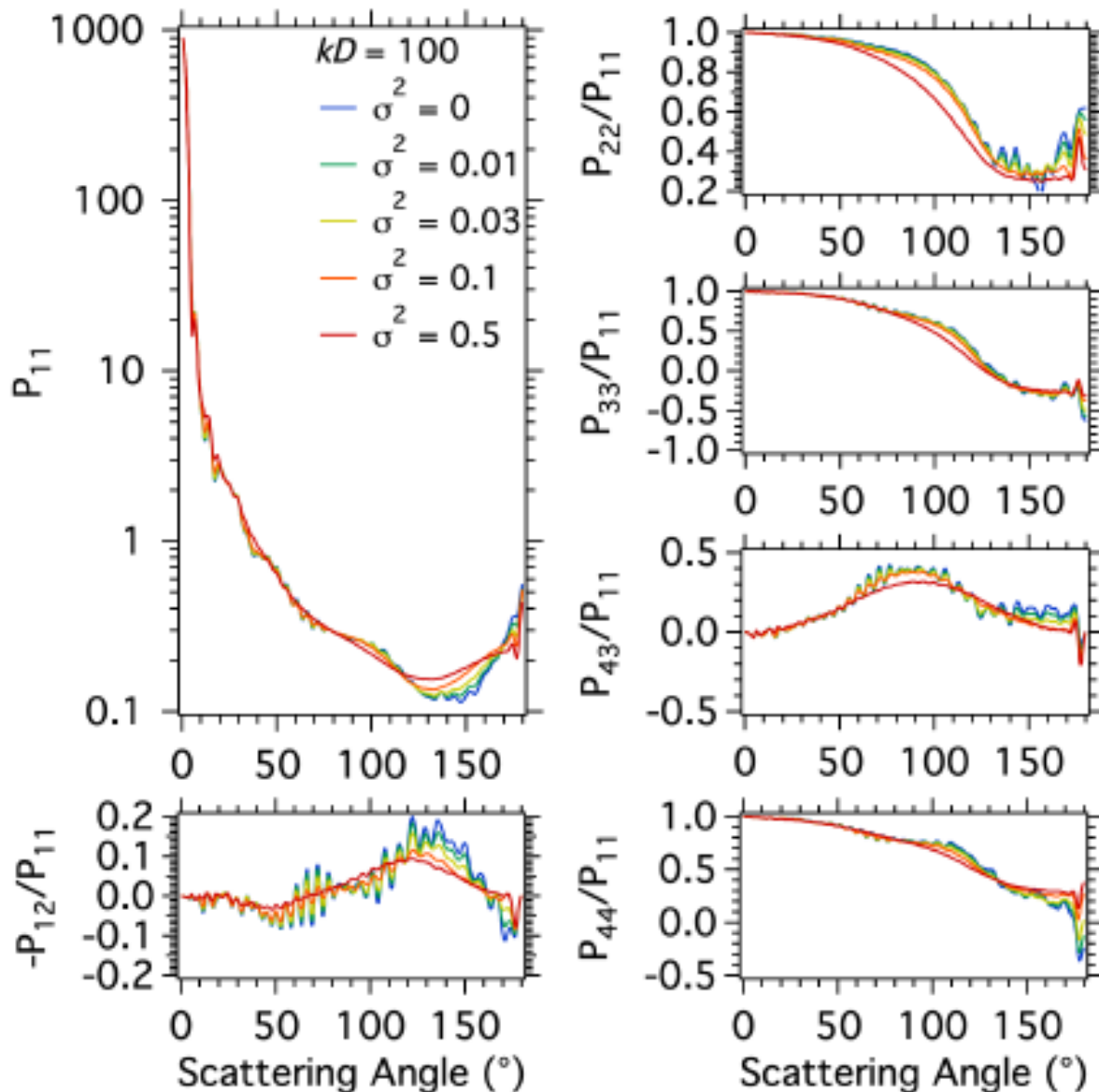


Figure 2. The phase matrix elements of hexagonal column particles with size parameter 100 and various degrees of surface roughness.

Figure 3 illustrates the impact of the relative scale of the surface texture of ice crystals. The phase matrix elements with the smallest number of faces (i.e., $kD_{\text{face}} = 10$) show noticeable differences, compared to the counterparts of other particles with smaller relative scales of the surface roughness. However, the phase matrix elements of ice crystals with $kD_{\text{face}} \leq 5$ are almost identical, implying that small-scale surface roughness relative to size parameters $kD_{\text{face}} > 5$ needs to be considered in the ice optical property modeling, but relative roughness scales smaller than $kD_{\text{face}} \leq 5$ are not optically important.

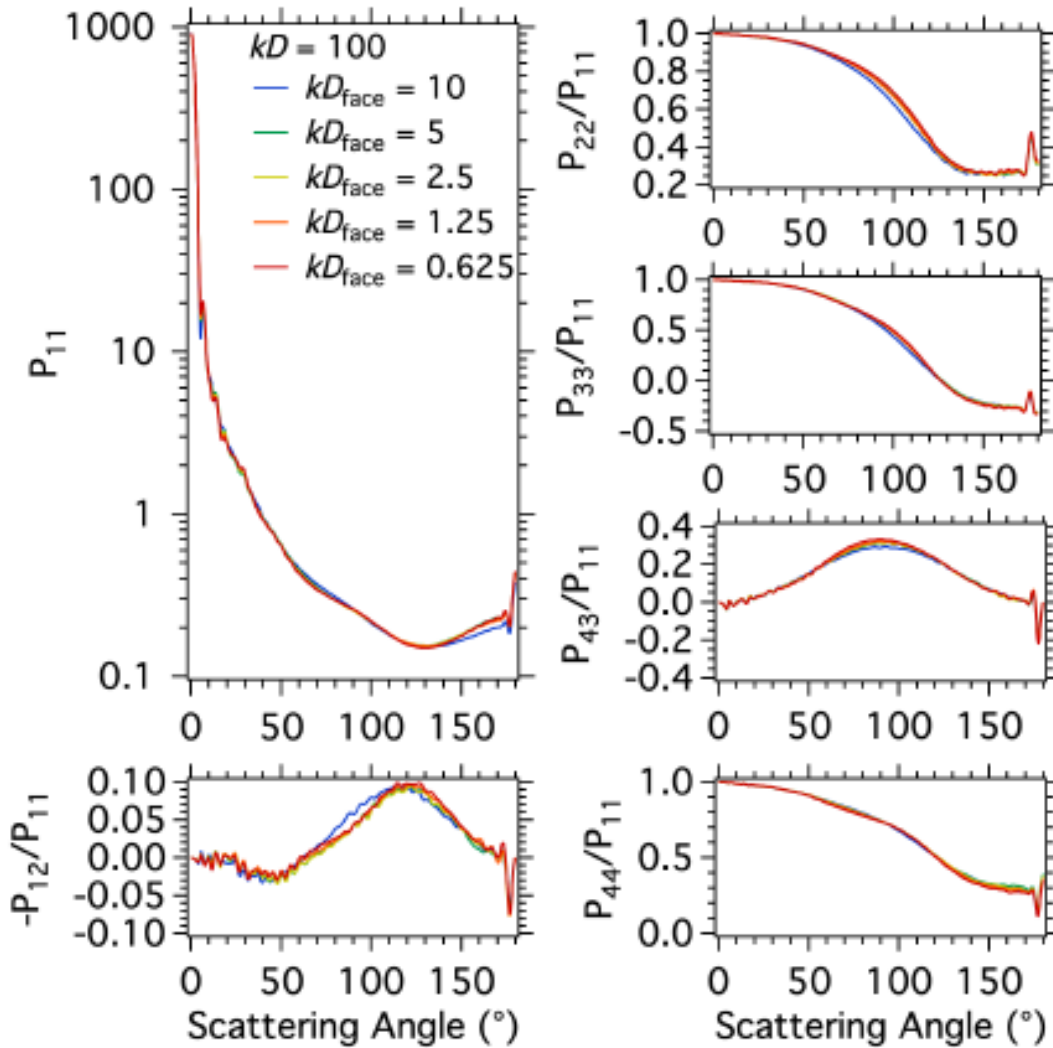


Figure 3. The phase matrix elements of hexagonal column particles with various relative scales of the surface roughness.

Figure 4 shows proposed ice crystal shapes to be used as part of the next-generation ice optical property model. According to the results from the sensitivity tests and literature survey, we will consider degrees of surface roughness ranging from 0–0.8 and aspect ratios ranging from 0.2–5, which includes both hexagonal plates and columns. Unlike previous studies, we will consider the effect of surface roughness on particles larger than size parameter 5. In the implementation of these ice crystal shapes into the next-generation ice optical property model, we will consider a weighted ensemble of individual particles.

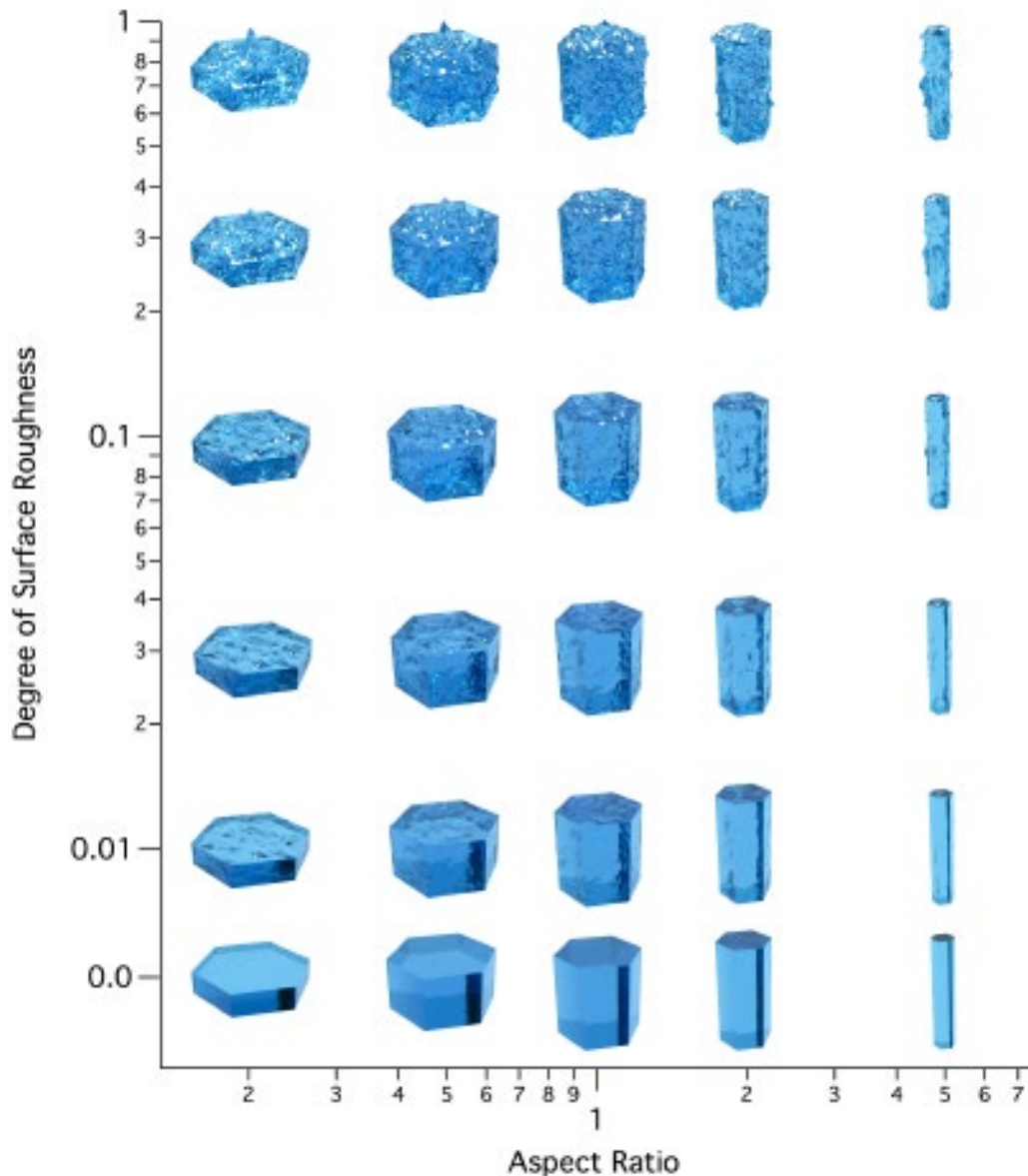


Figure 4. Ice crystal shape models to be used as part of the next-generation ice optical property model.

Task 2: Procedures and dataset for the consistency evaluations of the next-generation ice optical property model

- Collect GOES 16/17 and CALIPSO products as well as other complementary products;
- Develop the GOES 16/17 forward models for the ice cloud property retrievals.

We combined Task 2 and Task 3 in the original proposal as one task because the retrieval process includes an optimization of the forward model based on a newly developed technique.

We have collected the satellite derived products and complementary datasets for the CONUS region for August 28th 2017 as a one-day test data base. Table 1 summarizes the collected datasets, which includes the GOES-16 level 1b (L1b) Radiance Product, level 2 (L2) Cloud and Moisture Imagery (CMI) product, Clear Sky Mask (CSM) product, Cloud Top Height (CTH) product, Land Surface Temperature (LST) product, and other complementary products such as the UW Baseline Fit Emissivity Database (BFED) (Seemann et al. 2008), MERRA-2, CALIOP

L2 cloud layer (CLay) 1km product, MODIS level 3 (L3) 8-day-mean Sea Surface Temperature (SST) product, LST product, and Reflectance product. After finishing the development of the ice optical property model, we will collect these datasets for all other days in August 2017 for extensive validation.

Table 1: Summary of datasets in this project

Product	Satellite	Variable
L1b Radiance	ABI/GOES-16	Radiance
L2 CMI	ABI/GOES-16	Cloud reflectance and Brightness temperature
L2 CSM	ABI/GOES-16	Cloud masks
L2 CTH	ABI GOES-16	Cloud top height/temperature/pressure
L2 LST	ABI/GOES-16	Land surface temperature
BFED	MODIS/Aqua-Terra	Land surface emissivity
MERRA-2	N/A	Atmospheric temperature/gas profile
L2 Clay 1km	CALIOP/CALIPSO	Vertical Feature Mask, backscatter
L3 8-day SST	MODIS/Aqua-Terra	Sea surface temperature
L3 LST	MODIS/Aqua-Terra	Land surface temperature/emissivity
L3 Reflectance	MODIS/Aqua-Terra	Land surface reflectance

We have made substantial efforts to build the forward models of the GOES-16/17 and CALIOP sensors, which will be incorporated into the retrieval system to conduct the consistency evaluations. In the first 6 months, we have built a CALIOP sensor simulator and associated look-up-table (LUT) for existing ice optical property models including MODIS Collection 6 and the Two-Habit Model (THM). In addition, the GOES-16/17 ABI simulators for particular bands are currently under development, including visible, near-infrared for the Nakajima–King ice cloud property retrieval (Nakajima and King, 1990), and thermal infrared split-window bands for the split-window ice cloud property retrieval.

University of Michigan accomplishments:

The University of Michigan (UM) co-I has assessed the performance of CRTM2.4.0 with benchmark line-by-line radiative transfer model (LBLRTM12.0; Clough et al., 2005) and another widely used radiative transfer model in Earth remote sensing community, Moderate Transmission Code version 5 (MODTRAN5; Anderson et al., 2007). As the first step of the assessment, only clear-sky cases are considered. Based on the GEOS-16 and GOES-17 ABI spectral response functions for all infrared channels (i.e. wavelength > 4um), we used three radiation transfer models to simulate the ABI radiances in these channels for a typical clear-sky tropical profile (McClatchey et al., 1972) and for the US 1976 standard atmosphere profile. The results from two profiles are similar, and the detailed comparisons for the tropical profile are shown in Fig. 5. The brightness temperature (BT) differences between the CRTM2.4.0 and LBLRTM12.0 are all within ± 1.5 K except for the 9.6um channel, which has a difference as large as 3K in BT. For the US 1976 standard atmosphere profile, the difference between the CRTM2.4.0 and LBLRTM12.0 for the 9.6um channel is about 1K in BT, also the largest among differences in all channels. The major clear-sky absorption feature in the 9.6um channel is ozone and the surface emissivity in three simulation is identical, thus it is likely that the

difference is due to how the CRTM 2.4.0 parameterized ozone absorptions. Note the agreements between CRTM2.4.0 and MODTRAN5 is better than the agreements between CRTM2.4.0 and LBLRTM12.0, which might reflect common challenges in parameterizing ozone absorption in such fast radiative transfer models.

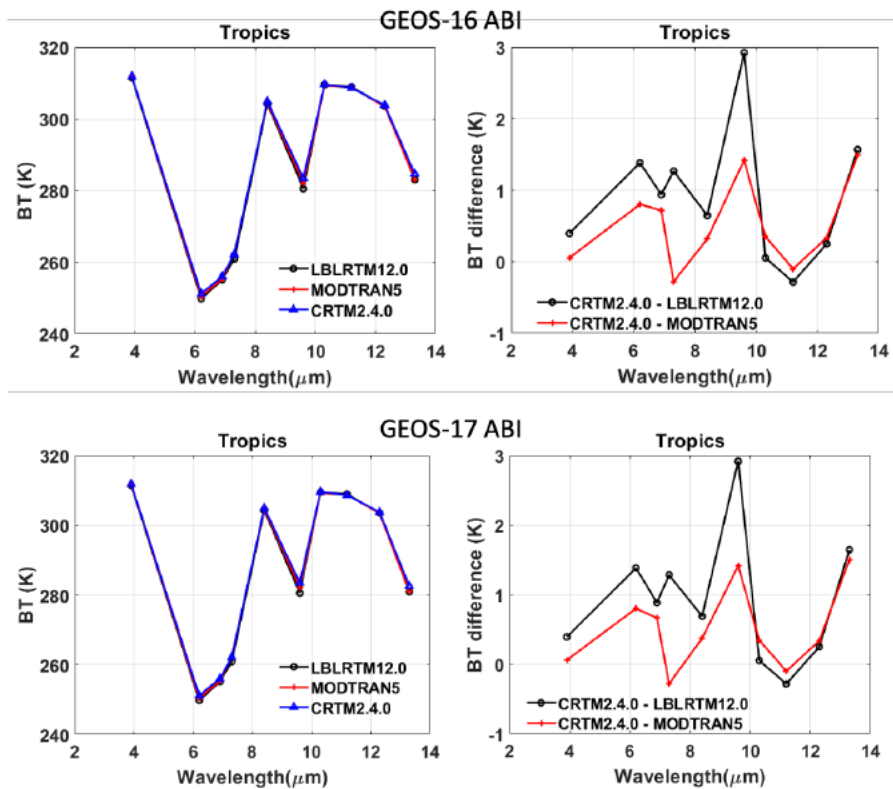


Figure 5. Upper right panel: the simulated brightness temperatures at GEOS-16 ABI infrared channels for clear-sky tropical profile by three RTMs, CRTM2.4.0, LBLRTM12.0, and MODTRAN5. Upper left panel: the difference between CRTM2.4.0 and LBLRTM12.0 as well as the difference between CRMT2.4.0 and MODTRAN5. Lower panels: same as the upper panels except for GEOS-17 ABI.

Plans for Next Reporting Period

For the next 6 months, we will compute the single-scattering properties of ice crystals at the single-particle level for wide ranges of particle sizes and wavelengths, which will be used to develop a next-generation ice optical property model. In addition, we will finalize a retrieval system to perform the consistency check in ice cloud property retrievals using GOES-16/17 and CALIOP observations.

The University of Michigan co-I, Prof. Xianglei Huang, will further understand the issue of CRTM clear-sky simulation for the 9.6μm channel. Meanwhile, Prof. Xianglei Huang implemented the most recent ice cloud scattering database developed by the PI to MODTRAN5. Modtran5 has flexibility of specifying DISORT solver up to 64 streams, which makes it capable of accurately modeling scattering cloudy radiances. Prof. Huang plans to use this to evaluate the CRTM simulated cloudy radiances at the ABI infrared channels.

References

Anderson, G. P., A. Berk, J. H. Chetwynd, J. Harder, J.M. Fontenla, E.P. Shettle, et al.,

2007: Using the MODTRAN™5 radiative transfer algorithm with NASA satellite data: AIRS and SORCE. Proc. SPIE, 6565, 65651O.

<http://dx.doi.org/10.1117/12.721184>.

Bi L, and P. Yang 2014: Accurate simulation of the optical properties of atmospheric ice crystals with invariant imbedding T-matrix method. *J Quant Spectrosc Radiat Transf.* 138, 17–35

Clough, S. A., M. W. Shephard, E. J. Mlawer, J. S. Delamere, M. J. Iacono, K. Cady-Pereira, S. Boukabara, and P. D. Brown, 2005: Atmospheric radiative transfer modeling: A summary of the AER codes, *J. Quant. Spectrosc. Radiat. Transfer*, 91, 233–244, <https://doi.org/10.1016/j.qsr.2004.05.058>.

Korolev, A., and G. Isaac, 2003: Roundness and aspect ratio of particles in ice clouds. *J. Atmos. Sci.*, 60, 1795–1808.

Liu, C., Panetta, R. L., and Yang, P.: The effects of surface roughness on the scattering properties of hexagonal columns with sizes from the Rayleigh to the geometric optics regimes, *J. Quant. Spectrosc. Radiat. Transf.*, 129, 169–185, 2013.

Loeb, N. G., Yang, P., Rose, F. G., Hong, G., Sun-Mack, S., Minnis, P., Kato, S., Ham, S., Smith, W. L., Hioki, S., & Tang, G. (2018), Impact of ice cloud microphysics on satellite cloud retrievals and broadband flux radiative transfer model calculations. *J. Clim.*, 31, 1851–1864, <https://doi.org/10.1175/JCLI-D-17-0426.1>.

Magee, N., Boaggio, K., Staskiewicz, S., Lynn, A., Zhao, X., Tusay, N., Schuh, T., Bandamede, M., Bancroft, L., Connolly, D., Hurler, K., Miner, B., and Khoudary, E.: Captured Cirrus Ice Particles in High Definition, *Atmos. Chem. Phys. Discuss.* [preprint], <https://doi.org/10.5194/acp-2020-486>, in review, 2020.

McClatchey, R., R. Fenn, J. Selby, F. Volz, and J. Garing, 1972: Optical properties of the atmosphere. Tech. Rep. AFCRL-72-0497, AFGL(OPI), Hanscom AFB, MA 01731.

Nakajima, T., & King, M. D. (1990). Determination of the optical thickness and effective particle radius of clouds from reflected solar radiation measurements. Part I: Theory. *Journal of the Atmospheric Sciences*, 47(15), 1878–1893. [https://doi.org/10.1175/1520-0469\(1990\)047<1878:DOTOTA>2.0.CO;2](https://doi.org/10.1175/1520-0469(1990)047<1878:DOTOTA>2.0.CO;2)

Seemann, S. W., Borbas, E. E., Knuteson, R. O., Stephenson, G. R., & Huang, H. L. (2008). Development of a global infrared land surface emissivity database for application to clear sky sounding retrievals from multispectral satellite radiance measurements. *J. Appl. Meteor. Climatol.*, 47(1), 108–123. <https://doi.org/10.1175/2007JAMC1590.1>.

Um, J., G. M. McFarquhar, Y. P. Hong, S.-S. Lee, C. H. Jung, R. P. Lawson, and Q. Mo, 2015: Dimensions and aspect ratios of natural ice crystals. *Atmos. Chem. Phys.*, 15, 3933–3956, doi:10.5194/acp-15-3933-2015.

Voigtländer, J., and Coauthors, 2018: Surface roughness during depositional growth and sublimation of ice crystals. *Atmos. Chem. Phys.*, 18, 13 687–13 702,

<https://doi.org/10.5194/acp-18-13687-2018>.

Yang, P. and K. N. Liou, 1998: Single-scattering properties of complex ice crystals in terrestrial atmosphere, *Contr. Atmos. Phys.*, 71 (2), 223–248.

Yang, P., L. Bi, B. A. Baum, K. N. Liou, G. L. Kattawar, M. I. Mishchenko, and B. Cole, 2013: Spectrally consistent scattering, absorption, and polarization properties of atmospheric ice crystals at wavelengths from 0.2 to 100 μm , *J. Atmos. Sci.*, 70, 330–347.

Zhang, J., Bi, L., Liu, J., Panetta, R.L., Yang, P., Kattawar, G.W., 2016. Optical scattering simulation of ice particles with surface roughness modeled using the Edwards-Wilkinson equation. *J. Quant. Spectrosc. Radiat. Transfer* 178, 325–335. doi:10.1016/j.jqsrt.2016.02.013.